An edge detection algorithm for imaging ladar

Qi Wang (王 骐), Ziqin Li (李自勤), Qi Li (李 琦), Jianfeng Sun (孙剑峰), and Juncheng Fu (傅俊诚)

National Key Laboratory of Tunable Laser Technology, Institute of Opto-Electronics, Harbin Institute of Technology, Harbin 150001

Received December 16, 2002

In this paper, the morphological filter based on parametric edge detection is presented and applied to imaging ladar image with speckle noise. This algorithm and Laplacian of Gaussian (LOG) operator are compared on edge detection. The experimental results indicate the superior performance of this kind of the edge detection.

OCIS codes: 100.2000, 110.1650, 110.3080, 280.3640.

For years, there has been much interest in the field of laser radar owing to its three-dimensional, high-resolution imagery and effectiveness at anti-jamming. However, the images produced by coherent detection are affected by signal-dependent noise known as speckle. Speckle-reduction and identification of the image information has become an active research field[1−4]. Generally, conventional edge detection algorithms comprise two main processing elements: speckle reduction and edge detection.

Conventional edge detectors carry out the edge-detection by introducing differential operator or high-pass filters in frequent domain, which is very sensitive to noise and causes false edge. In addition, the processing of speckle reduction needs a lot of time. As a result, the edge detectors based on a prior knowledge of statistical character of speckled image gray distribution have been developed. These algorithms can be applied to detect edges without image preprocessing for speckle suppression and save time significantly. For example, parametric test operator presented by K. D. Donohue *et al.*[5], rate edge detector presented by R. Touzi *et al.*[6,7], and the Student t test by R. Cook *et al.*[8,9].

In this paper, we present the morphological filter based on parametric edge detection[5]. Both our approach and conventional Laplacian of Gaussian (LOG) detector are applied to ladar image corrupted by speckle, and the experimental results indicate that ours has the superior performance.

It is well known that speckle is a multiplicative noise[10] and has the statistical features of the negative exponential density. Speckle-degraded images can be expressed by

$$I_{i,j} = x_{i,j} n_{i,j}, \tag{1}$$

$$p(n_{i,j}) = \exp(-n_{i,j}), \tag{2}$$

where $I_{i,j}$ is the measured intensity of the i,jth pixel, $x_{i,j}$ is the true scattering intensity associated with the underlying scatters of the illuminated scene, $n_{i,j}$ is the intensity affected by speckle noise, and $p(n_{i,j})$ is the probability of speckle.

There are three cases in a suitable window which images exist: target, background and boundary region. In boundary region where edge exists, there are two regions which have different statistics. R_0 denotes the region of pixels with a sample mean x_0, and R_1 denotes a set of pixels from a neighboring region with a sample mean intensity x_1. An edge is defined as the boundary between two neighboring pixel regions associated with different statistics. Let the null hypothesis H_0 denote the case in which pixels from R_1 have the same statistics as those in R_0[8]. And edge detection is used to decide whether or not the null hypothesis H_0 is accepted. If H_0 is accepted, there are the same statistics between R_0 and R_1, and the center pixel of the window is not part of the edge.

In practice, because the mean intensity values from local regions R_0 and R_1 are not known, they can be determined from the maximum-likelihood estimate[11],

$$\bar{x}_k = \frac{1}{N_k} \sum_{i,j \in R_k}^{N_k} I_{i,j}, \qquad k = 0, 1, \tag{3}$$

where N_k is the number of pixels in R_k.

We can select bigger windows, but the increment of the size of window will result in the decrement of the detective probability[5]. And considering the fewer pixels of the ladar images (32×64), it is enough to select the 3×3 window. Two pixel regions R_0 and R_1 can be formulated such that they are divided along a vertical, a horizontal, 135° and 45° diagonal edges, as the enclosed regions shown in Figs. 1(a), (b), (c), and (d), respectively.

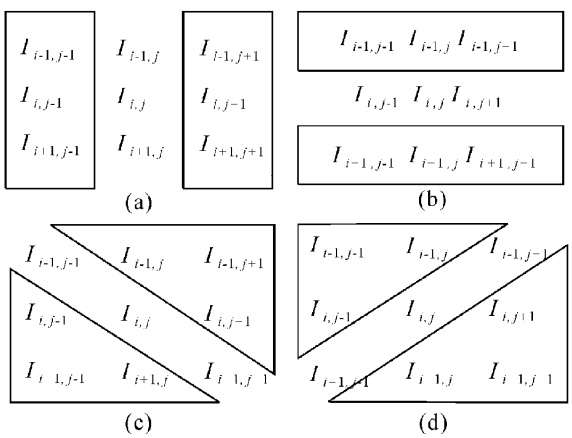

Fig. 1. Local pixel neighborhoods R_0 and R_1 for determining the presence of an edge.

Considering randomness of $\bar{x}_0$ and $\bar{x}_1$, if sample mean $\bar{x}_0$ is less than or equal to sample mean $\bar{x}_1$, the edge detection function is expressed as

$$TF(\bar{x}_0, N_0, \bar{x}_1, N_1) = 1 - P(N_1\bar{x}_1|H_0) + P(N_0\bar{x}_0|H_0), \tag{4}$$

where $P(N_k\bar{x}_k|H_0)$ is the probability of R_k having a mean less than $\bar{x}_k$, assuming H_0 is true. As the distribution of the sum of independent and identically distributed exponential random variables is the gamma distribution, $P(N_k\bar{x}_k|H_0)$ may be obtained by gamma function.

Meaning of the edge detection function is the area of the shadow in Fig. 2. Given a significance level, or a desired false-alarm probability (P_{FA}). If the value of the edge detection function is above the significance level, it shows the similarity of $\bar{x}_0$ and $\bar{x}_1$, i.e. H_0 is accepted. Then the center pixel of the window $I_{i,j}$ is not a pixel of edges, if not, H_0 is rejected, $I_{i,j}$ is a pixel of edges.

$$TF(\bar{x}_0, N_0, \bar{x}_1, N_1) \begin{cases} \leq P_{\mathrm{FA}} & \text{reject } H_0 \quad \text{(edge)} \\ > P_{\mathrm{FA}} & \text{accept } H_0 \quad \text{(no edge)} \end{cases}. \tag{5}$$

There are four pairs of R_0 and R_1 in each window. $TF(\ )$ in Eq. (4) is the minimum value of four values. So the edges are detected.

The morphological filter is a usual way on the binary image. The primary morphological operations are dilation and erosion whose implements are based on the concept of filling the structuring elements. Erosion and dilation create two important morphological transformations called opening and closing. The opening of an image A by the structuring element B is denoted by $A \circ B$. The closing of an image A by the structuring element B is denoted by $A \bullet B$. The "salt and pepper" noise in the background can be removed by opening. The "sand hole" noise in the images can be removed by closing.

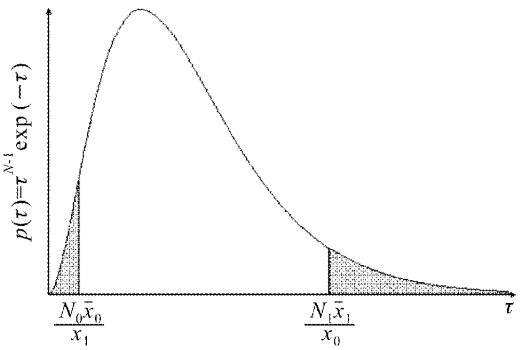

Fig. 2. Test function.

There are isolated erroneous test points in the image BW processed by parametric test detector. These points are tantamount to the "salt and pepper" noises. Therefore, we first use the structural elements

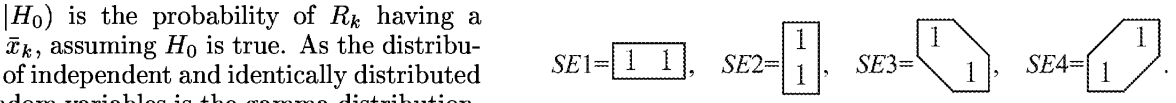

to finish opening for the image BW respectively, then operate union (∪) on four images to obtain final edge image BW'.

$$BW1 = BW \circ SE1, \quad BW2 = BW \circ SE2,$$
$$BW3 = BW \circ SE3, \quad BW4 = BW \circ SE4, \tag{6}$$
$$BW' = BW1 \cup BW2 \cup BW3 \cup BW4. \tag{7}$$

By morphological filter, most isolated missing pixels in edge image background can be removed. Thus, the error of the edge detection can bring down exceedingly and be useful to subsequent processing (such as edge link).

To test the performance of our new edge detection algorithm based on the combination of parametric test detector and morphological filter, we applied it to the speckle degraded image derived from pulsed CO_2 laser active imaging system based on heterodyne detection.

The block diagram of imaging ladar is shown in Fig. 3. The ladar is composed of a pulsed transmitter laser, a CW local oscillator, a monostatic optical system, a 2-D scanner, a coherent heterodyne detector, and signal processor etc. The signal processor gives 2-D digital image.

Figure 4(a) is a photo of the illuminated target (a building) made up of red bricks, and Fig. 4(b) is the 256 gray-level image (32 × 64 pixels) derived from the laser imaging system image. Although many windows of the building can be seen in the photo, they are too small in size to resolve power of our laser imaging system. Figure 4(c) is the result by parametric test detector. Let the value for significance level be 0.1 to reduce probability of false-alarm (P_{FA}). Figure 4(d) is the result derived from our new edge detector. It is clear that the edge detection in Fig. 4(d) is better than that in Fig. 4(c). LOG operator is usually used for edge detection[12,13]. Figure 4(e) is the result by LOG operator. The edge in Fig. 4(e) is confused.

From Fig. 4, our new approach based on the combination of parametric test detector and morphological filter performs better than other algorithms for image derived

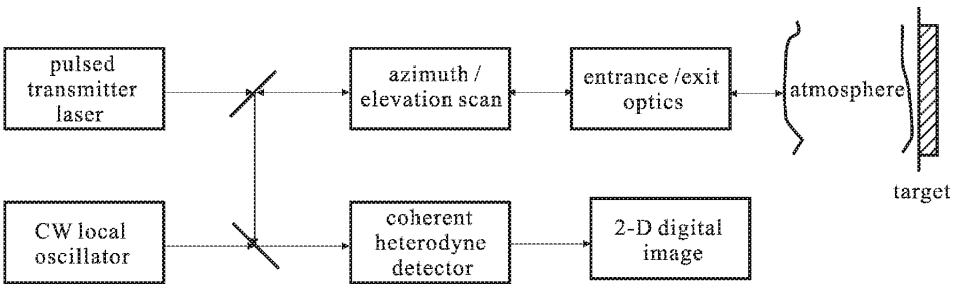

Fig. 3. Block diagram of a coherent imaging ladar.

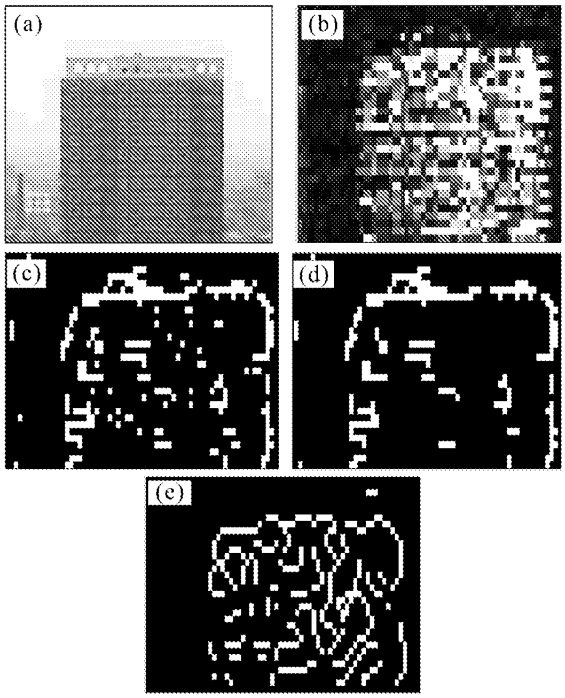

Fig. 4. Processing results of imaging ladar image. (a) Object photograph; (b) imaging ladar image; (c) result of edge detection; (d) morphological filtering based (c); and (e) LOG operator.

from laser active imaging system while P_{FA} is relatively low.

In this paper, a modified version of edge detector is developed for speckle-degraded image based on the combination of the parametric test detector and the morphological filter. The experimental results indicate the superior performance of this kind of the edge detection. From the result above, there are still some false edges in edge image and it is our future work to detect more true edges and reduce false edges at the same time.

Z. Li is the author to whom the correspondence should be addressed, his e-mail address is cqlziqin@0451.com.

References

1. L. H. Jiang, C. H. Wang, and Q. Wang, Chin. J. Laser B **9,** 182 (2000).
2. L. H. Jiang, C. H. Wang, and Q. Wang, Acta Optica Sinica (in Chinese) **20,** 1623 (2000).
3. S. Fukuda and H. Hirosawa, INT. J. Remote Sensing **19,** 507 (1998).
4. D. M. Smith, INT. J. Remote Sensing **17,** 2043 (1996).
5. K. D. Donohue, M. Rahmati, L. G. Hassebrook, and P. G. Krishnan, Optical Engineering **32,** 1935 (1993).
6. R. Touzi, A. Lopes, and P. Bousquet, IEEE Trans. on Geoscience and Remote Sensing **26,** 764 (1988).
7. A. C. Bovik, IEEE Trans. on Acoustics Speech and Signal Processing **36,** 1618 (1988).
8. R. Cook, I. McConnell, D. Stewart, and C. Oliver, Proc. SPIE **2316,** 92 (1994).
9. C. J. Oliver, D. Blacknell, and R. G. White, IEE Proc.: Radar Sonar Navig **143,** 31 (1996).
10. J. C. Dainty (ed.), translated by L. T. Huang, T. J. Wang, S. Y. Lin, *Laser Speckle and Related Phenomena* (in Chinese) (Science in China Press, Beijing, 1981) pp. 1 – 8.
11. P. L. Meyer (ed.), translated by K. R. Pan, *Introductory Probability and Statistical Application* (in Chinese) (Higher Education Press, Beijing, 1986) pp. 371 – 382.
12. D. Marr and E. Hildreth, Proc. R. Soc. Lond. B **207,** 187 (1980).
13. A. Huertas and G. Medioni, IEEE Trans. on Pattern Analysis and Machine Intelligence **PAMI-8,** 651 (1986).